ORIGINAL ARTICLE

Susceptibility assessments of the Wenchuan earthquake-triggered landslides in Longnan using logistic regression

S. B. Bai · J. Wang · B. Thiebes · C. Cheng ·
Z. Y. Chang

Abstract In this study a Wenchuan earthquake-induced landslide susceptibility assessment was carried out in the Longnan area in northwestern China using a GIS-based logistic regression model. This region has frequently been affected by landslides in the past, and was intensively affected by the 5.12 Wenchuan earthquake which received considerable international attention. The data used for this study consist of the landslides triggered by the Wenchuan earthquake and a landslide pre-disposing factor database. Information regarding the landslide causative factors came from additional data sources, such as a digital elevation model (DEM) with a 30×30 m^2 resolution, orthophotos, geological and land-use maps, precipitation records, and information on peak ground acceleration data from the 2008 earthquake. The statistical analysis of the relationship between the Wenchuan earthquake-triggered landslides and pre-disposing factors showed the great influence of lithological and topographical conditions on slope failures. The quality of susceptibility mapping was validated by splitting the study area into training and validation sections. The prediction capability analysis demonstrated that the landslide susceptibility map could be used for land planning as well as emergency planning by local authorities.

S. B. Bai (✉) · J. Wang · B. Thiebes · C. Cheng · Z. Y. Chang
Key Laboratory of Virtual Geographic Environments (National Education Administration), College of Geographical Sciences, Nanjing Normal University, Nanjing 210046, China
e-mail: shibiaobai21@163.com

Introduction

Earthquake-triggered landslides are very common throughout the world. In particular, the last large earthquake events, e.g. in Pakistan in 2005 and in China in 2008, have demonstrated the importance of seismic shaking for the initiation of slope failures. For instance, the 2008 Wenchuan earthquake (magnitude 8.0) shook the area located in the mountainous region of northwest of Sichuan Province. It brought overwhelming destruction to eight provinces and cities, including Sichuan, Gansu, Shanxi, Chongqing, Yunnan, Shaanxi, Guizhou, and Hubei. The area is characterized by rugged topography, steep high mountains, deep valleys, and complicated geologic structures. The Wenchuan earthquake induced more than 15,000 landslides, debris flows, and rock avalanches in an area of about 50,000 km^2, and it is estimated that approximately 20,000 deaths were directly related to these landslides (Huang and Li 2008; Yin et al. 2009). From the landslides and debris flows within the Wenchuan earthquake area, related risks can be observed at up to 12,700 locations, threatening the lives of almost one million people (Huang and Li 2008; Cui et al. 2009; Yin et al. 2009). The earthquake also destabilized many slopes and produced large amounts of material for future landslide events. Consequently, it is estimated that debris flows and landslides will occur at higher intensity and with higher frequency than normal; the occurrence of debris flows triggered by the heavy rainfall of 24 September 2008 indicates that the Wenchuan earthquake areas are now particularly susceptible to debris flows which are likely to

occur frequently within the next 5–10 years (Tang et al. 2009). It has been suggested that the impact of an earthquake can increase the activity of landslides and debris flows for a period of 10–30 years (Cui et al. 2008; Xie et al. 2009). This can be expected to impact significantly local land use, planning and construction, and will restrict the future development of the area.

It will usually be appropriate to carry out landslide susceptibility zoning as a first stage in the development of landslide hazard or risk zoning for planning purposes (Fell et al. 2008). The frequent occurrence of landslides, collapses, and breakdowns in the Longnan region brought about a major effect on land planning and post earthquake construction, and became an obstacle to the sustainable development of the local economy. At the moment, the local and regional authorities at Longnan rely primarily on landslide inventory maps to conduct spatial planning and to organize emergency actions. It is, therefore, essential to provide more reliable landslide susceptibility maps to facilitate landslide hazard and risk management in the region. Although it is expected that landsliding will occur more frequently in the most susceptible areas, in the susceptibility analysis the time frame is not taken into account explicitly (Fell et al. 2008). Furthermore, the susceptibility maps are on a regional scale and cannot be used for site-specific work or as a substitute for professional advice from qualified geologists or geotechnical engineers.

In order to determine the most fragile landslide areas in the future under the influence of a similar earthquake, it is important to determine the areas prone to future landslide, through landslide-susceptibility maps. Both qualitative and quantitative methods have been used in the processes of creating landslide-susceptibility maps (Soeters and Van Westen 1996; Aleotti and Chowdhury 1999; Guzzetti et al. 1999; Xu et al. 2012a, b). Qualitative methods were widely used during the late 1970s by engineering geologists and geomorphologists. Quantitative methods, however, have become popular in the past few decades largely because of their numerical expressions of the relationship between controlling factors and landslides, assisted by the advances in computer and geographic information system (GIS) technology (Dai et al. 2001; Dai and Lee 2002; Chung et al. 2002; Van Westen and Getahun 2003; Van Westen et al. 2008; Bell and Glade 2004; Guzzetti et al. 2005; Bai et al. 2011; Dai et al. 2011; Xu et al. 2012b). The logistic regression (LR) method has been applied extensively to landslide susceptibility mapping (e.g. Atkinson and Massari 1998; Guzzetti et al. 1999; Bai et al. 2010; Yalcin et al. 2011). The algorithm of logistic regression applies maximum likelihood estimation after transforming the dependent variable into a logical variable, representing whether the natural log of odds of the dependent variable occurs or not.

The purpose of this study was to analyze the relation between Wenchuan earthquake-triggered landslides and pre-disposing factors and to carry out landslide susceptibility assessments by logistic regression in Longnan.

The study area

The study area, Longnan, is located in the southeast of Gansu Province in China (Fig. 1). In total, it covers an area of approximately 27,000 km². The region is mountainous and has a large relief varying between 550 m and more than 4,000 m above sea level. The administrative unit includes one district and eight counties organized in 193 towns and townships, inhabited by 2.7 million people. Longnan is located in the transition zone between the Tibetan Plateau and the Loess Plateau, of which a large area is covered by extensive loess deposits. The Tibetan Plateau uplift has resulted in a high geomorphic activity. Two metamorphic rock units (the Bailongjian and the Bikou) have been identified. The Bailongjiang metamorphics are exposed in the northwestern quadrant of this region and consist of conglomerates, slates, limestones, and phyllites. The metamorphic rocks belonging to Bikou unit are located in the south, and consist of igneous rocks, phyllites, and slates (Derbyshire et al. 2000). The geological structures are dominated by the southern Qinling fold system. During the geologically recent Yenshan and Himalayan crustal movements, uplift and complex faulting of the region took place, resulting in widespread valley incision and undercutting of the slopes. About 90 % of the area north of the Bailongjiang River is mountainous. Here, the Qinling Mountains are segmented by two branches from the Bailongjiang River, the Dieshan in the north and the Minshan in the south. Such severe incision has resulted in high relative relief and a landscape marked by many large landslides. The combination of frequent earthquakes, high relative relief, steep slopes, strongly seasonal monsoonal climates, and widely distributed thick loess results in both large single failures and widespread landslide occurrence.

The Longnan region is one of the four most active landslide and debris flow regions in China, characterized by a very high frequency of occurrence (Scheidegger and Ai 1987). Figure 1 presents the peak ground acceleration (PGA) in the study area. According to the China Geological Survey Bureau of Statistics (2008), geological disasters killed 567 people in the 40 years before the Wenchuan earthquake. The geological hazards induced by the Wenchuan earthquake killed further 147 people, injured 468, and caused a direct economic loss of 2.855 billion Yuan (0.41 billion $).

Data

Several data sources were utilized for the investigations of landslide pre-conditioning environmental factors and the

Fig. 1 Location of the study area, Longnan
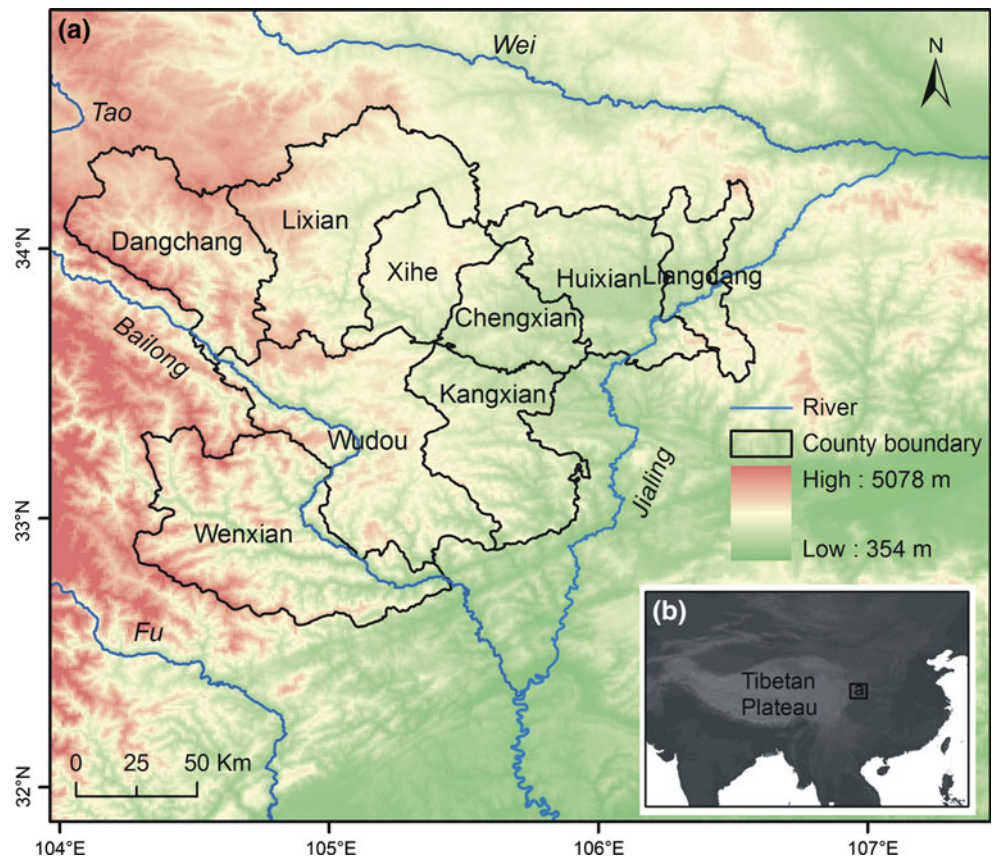
subsequent analysis of landslide susceptibility. All data sources are listed in Table 1.

Following the main shock of the Wenchuan earthquake, the Ministry of Land and Resources of China immediately organized scientists to conduct earthquake engineering and geological reconnaissance to provide scientific decision-making information and emergency countermeasures for the immediate post-seismic emergencies and also for the mid-term transitional resettlement sites and reconstruction. In order to gain reliable information on the seismogenic

geohazards, the investigation was based on two approaches: field investigation and remote-sensing image interpretation (Huang and Li 2008; Tang et al. 2009).

The typical landslide morphology recognizable on the available maps includes visible scarps, hummocky topography, and landslide dams. Different landslide types were summarized in terms of the following classes: rockfalls (including rock falls, debris falls and rock avalanches); landslides (debris slides and rotational slides, slump); and debris flows, according to Varnes's (1984) and Cruden and

Table 1 Data properties

Data	Format	Scale	Additional information	Source
Digital Elevation model	ArcGIS Grid	30 × 30 m	Digitized topographical map (1:50,000 scale)	Chinese Bureau of Cartography
Landslide data	Shape file points		2,238 landslides triggered by 2008 Wenchuan earthquake	Longnan Bureau of Land and Resources (2008) Qin et al. (2009)
Geology	Shape file	1:200,000	Simplified to 11 lithological classes	China Geological Survey and Chen et al. (2006)
Rainfall	Shape file		Interpolated data from 600 weather stations in China (1971–2005)	China meteorological administration
Land use	Shape file		Derived from the TM image interpretation	Environment and Ecological Science Data Center for West China
Peak ground acceleration	Shape file			National Strong Motion Observation Network System (NSMONS) and (Lu et al. 2010)

Varnes's (1996) classification. From the post-seismic emergencies report of the General Monitoring Station of Geological Environment of Gansu province (Longnan Bureau of Land and Resources 2008) and the remote sensing emergency survey in the Wenchuan earthquake area (Qin et al. 2009), a total of 2,238 earthquake landslides were identified in the study area (Fig. 2).

Lithology plays a key role in the distribution of landslides and is correlated with the properties of the slope-forming materials, such as rock-mass strength and structure. Based on the geological maps at 1:200,000 scale and geotechnical criteria, a simplified rock group map was produced from an original geological map considering the composition and structure of bedrock. Eleven rock groups were defined based on their composition and physical–mechanical characteristics (Chen et al. 2006; Table 2). Each rock group has similar geological properties and conditions. An overview on the 11 rock groups is presented in Fig. 3.

The pixel size of the digital elevation model (DEM) is 30×30 m^2 (Fig. 2). To store the information of these parameter maps in a uniform thematic database, the size of each pixel for all the products was set to 30×30 m, regardless of the scale of the original source. Indeed, this has to be carefully considered by following interpretation. The elevation, slope angle, aspect, plan curvature, and profile curvature are derived from the DEM using standard ArcGIS®, while the distance from slope failures to rivers was digitized from the 1:50,000 topographic map and the faults was digitized from the 1:200,000 geological maps.

Land- use types (Fig. 4) were mapped using preprocessed and enhanced Landsat TM 5 images. The analyzed images were then digitally processed to modify further the boundaries by supervised classification with ERDAS (Earth Resource Data Analysis System) software. The accuracy of the land-use interpretation was validated in the field.

Within this study, the PGA was selected as the main earthquake landslide-triggering factor (Fig. 5). PGA data were obtained from the earthquake strong-motion record of the National Strong Motion Observation Network System (NSMONS) (Lu et al. 2010). The NSMONS consists of permanent free-field stations, special observation arrays, mobile observatories, and a network management system. During the Wenchuan earthquake, over 1,400 components of acceleration records were obtained from 460 permanent free-field stations. In addition, three arrays for topographical effect and structural response of the main shock were observed in the network system.

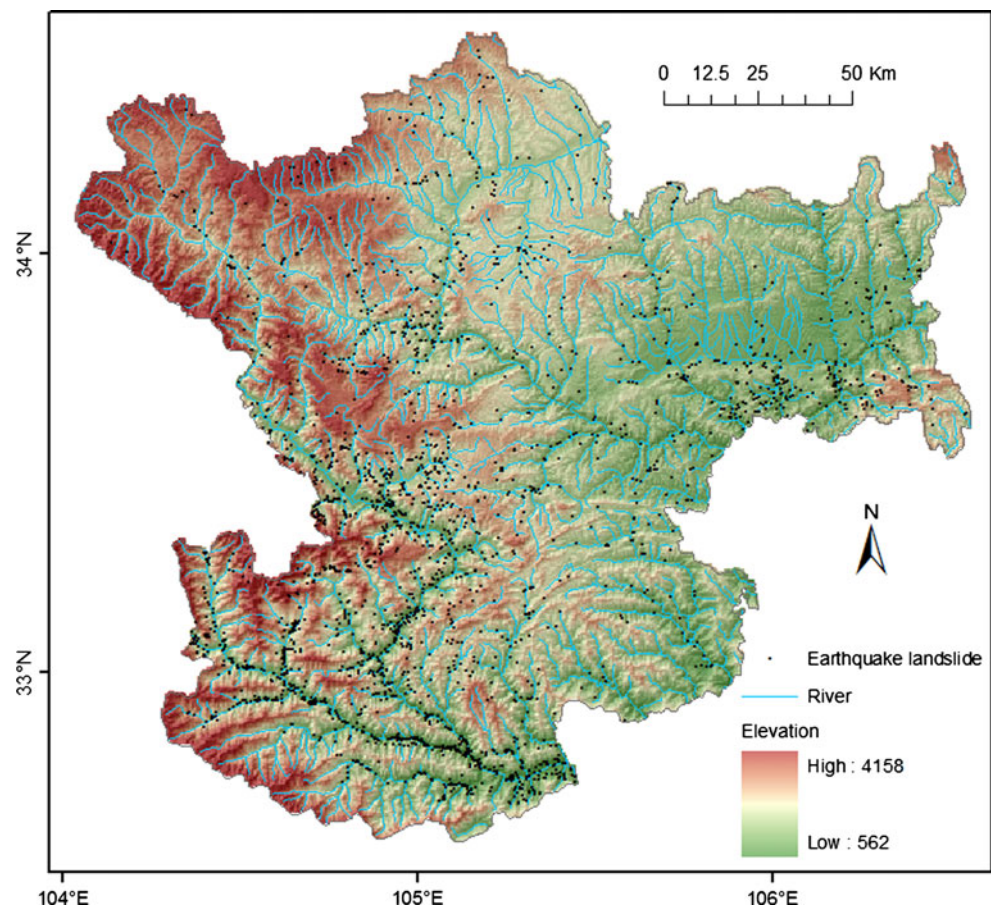Fig. 2 Elevation and spatial distribution of landslides in the study area

Table 2 Distribution of rock groups in the study area

Code	Rock group	Characteristics
A	Migmatite, gneiss, marble (Pt$_1$)	Biotite plagioclase migmatites, biotite monzonite migmatites, biotite K-feldspar migmatites, mixed quality of K-feldspar gneiss, marble folder, hornblende schist folder dolomitic marble
B	Metamorphic sandstone, metamorphic conglomerate, slate (DX, T$_1$b,T$_2$, T$_{2-3}$ T$_3$)	Metamorphic sandstone, sandy clay slate, sandstone, conglomerate, metamorphic fine sandstone, quartz sandstone
C	Metamorphic andesite, tuff metamorphic, metamorphic basalt (Pt$_{2-3}$, Ch, O$_{2-3}$, O$_3$)	Metamorphic andesite, andesitic basalt, andesitic tuff, basalt porphyry plus chert, tuffaceous sandstone, phyllite
D	Phyllite, slate, thin limestone (Qn, Z$_1$, S$_1$, S$_{2-3}$, D$_{1-2}$, D$_2$, D$_3$, P$_s$)	Phyllite mix quartzite, sericite phyllite mix tuff, carbonaceous phyllite mix slate, limestone, chert and fine and siltstone
E	Thick layer of limestone, slate (Jx, Z$_2$, S$_3$, D$_{2-3}$, C$_1$, C$_2$, C$_m$, P$_1$, P$_2$)	Thick layer of limestone rock in the splint, phyllite, chert, silty and fine sand, thick layer of slate, limestone, phyllite, chert and fine and siltstone
F	Thick layer of sandstone, limestone slate (€,T$_1$,T$_{1-2}$)	Thick layer of sandstone, slate phyllite, thin argillaceous limestone
J	Thick layer of conglomerate, sandy conglomerate (J$_1$, K$_1$, K$_2$, E$_2$)	Thick, thick layer of conglomerate, sandy conglomerate mudstones
H	Siltstone, mudstone, thin sandy conglomerate (J$_2$, E$_3$, N)	Muddy siltstone, silty mudstone in thin muddy sandstone, conglomerate, muddy sandstone
I	Rock sand and gravel (Qh)	Ancient river bed, modern bed alluvial, alluvial deposits of sand and gravel layers
J	Clay (Qp)	Loess, loess-like soil
k	Magmatic rocks (σ, ηγ, n, γ ,δo, βμ)	Granite, diorite, peridotite

Methodology

The methodology applied within this study includes a stepwise procedure. In a first step, the influence of landslide pre-conditioning environmental factors on landslide occurrence is analyzed. In a second step, landslide susceptibility is mapped by a logistic regression methodology, using the Wenchuan earthquake-triggered landslide.

Analyses of landslide pre-conditioning factors

The event-based earthquake landslide inventory was utilized within the study to investigate the influence of landslide pre-conditioning environmental factors. Two statistic variables were used: landslide density (LD) and landslide proportion (LP). The LD refers to the number of landslide points per km^2, while LP refers to the number of landslide points per each class of a pre-conditioning factor. The distribution of LD and LP is analyzed for rock groups, slope angle, aspect, land use classes, and distance to faults and rivers.
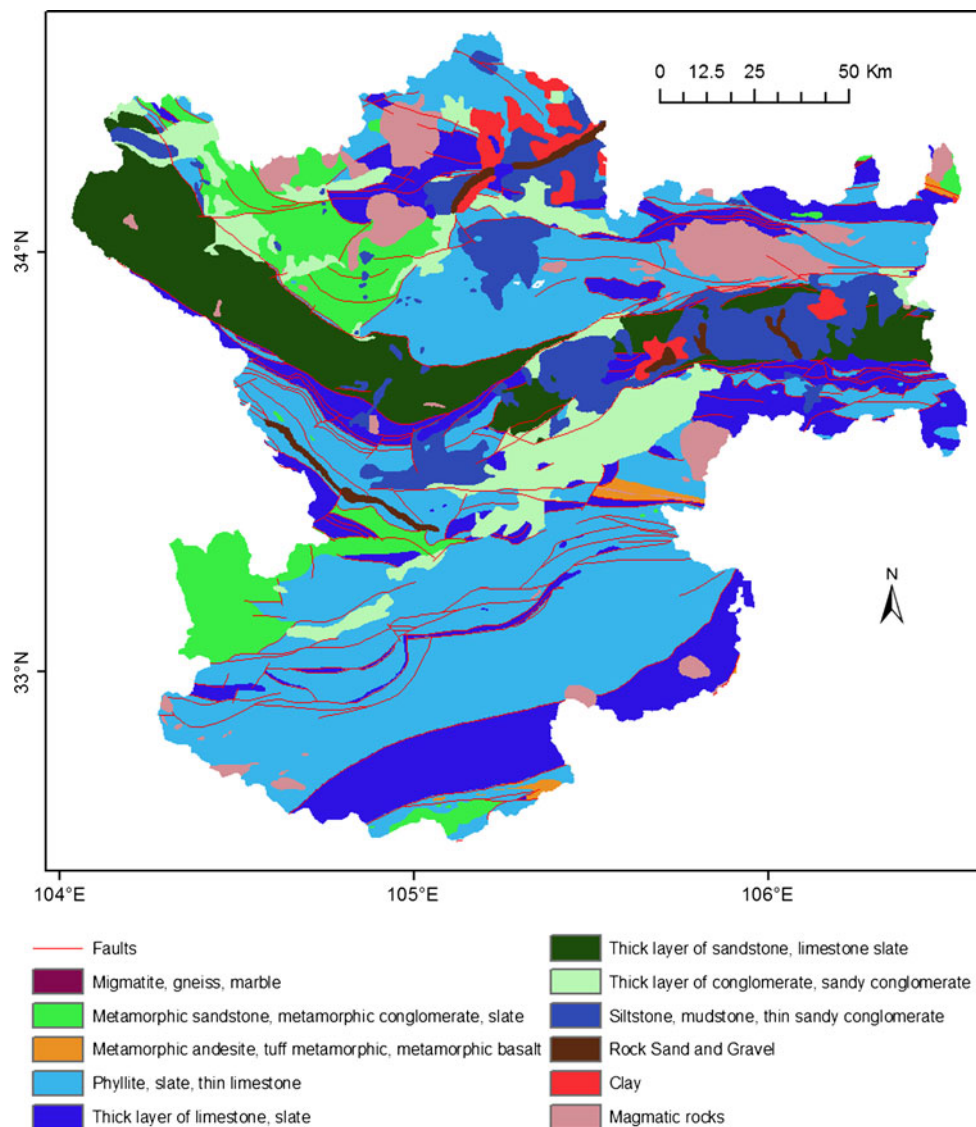
Mapping of landslide susceptibility

The basic concept of landslide susceptibility (Brab 1984; Chung and Fabbri 1999) includes the spatial distribution of factors related to the instability processes to determine zones of landslide-prone areas without any temporal implication. A landslide susceptibility map ranks the slope stability of an area in categories that range from stable to unstable and thereby show where landslides may occur (Chacon et al. 2006). Susceptibility may also include a description of the velocity and intensity of existing or potential landsliding (Fell et al. 2008). The identification and mapping of a suitable set of parameters related to landslide occurrence requires prior knowledge of their main causes (Guzzetti et al. 1999). The methodology applied in this study is based on the principle "the present and past are keys to the future". Although it can be questioned whether this principle is still valid in its generality, any study on this is beyond the presented research. The fundamental principle of this approach is to use the characteristics of existing landslides to evaluate possible areas for future landslides. In order to achieve this goal, databases including landslide characteristics and landslide causative factor were created and subsequently analyzed. Two major assumptions are made in a probabilistic approach of mapping susceptibility to landslides: (1) landslides will occur under similar environmental conditions to those in the past; and (2) predictions of which areas are likely to experience landslide in the future can be true only if the factors used for the forecasts will not change significantly in the future.

Logistic regression approach

The logistic regression estimates the probability of a certain event occurrence (Atkinson and Massari 1998). In the present situation, the dependent variable is a binary variable representing the presence or absence of landslides.

Fig. 3 Distribution of rock groups and faults in the study area

Faults

Migmatite, gneiss, marble

Metamorphic sandstone, metamorphic conglomerate, slate

Metamorphic andesite, tuff metamorphic, metamorphic basalt

Phyllite, slate, thin limestone

Thick layer of limestone, slate

Thick layer of sandstone, limestone slate

Thick layer of conglomerate, sandy conglomerate

Siltstone, mudstone, thin sandy conglomerate

Rock Sand and Gravel

Clay

Magmatic rocks

The logistic model can be expressed in its simplest form as follows:

$$P = \frac{1}{1 + e^{-z}} \quad (1)$$

where P is the probability of an event (landslide) occurrence, which varies from 0 to 1 on an s-shaped curve; z is defined as the following equation (linear logistic model), with its value varies from $-\infty$ to $+\infty$:

$$z = \hat{\beta}_o + \hat{\beta}_1 x_1 + \hat{\beta}_2 x_2 + \ldots + \hat{\beta}_n x_n \quad (2)$$

where $\hat{\beta}_0$ is the intercept of the model, n is the number of independent variables, $\hat{\beta}_i$ ($i = 1, 2, 3, \ldots, n$) is the slope coefficient of the model, and x_i ($i = 1, 2, 3, \ldots, n$) are the independent variables. This linear model is a logistic regression representing the presence or absence of landslides (at the present conditions) on the independent variables (pre-failure conditions).

Landslide susceptibility mapping using logistic regression

The landslide susceptibility calculation applied in this study is based on logistic regression includes four main steps: (1) splitting the dataset into a sampling and validation set; (2) multi-colinearity diagnosis; (3) application of logistic regression; and (4) validation and evaluation of the model results.

In logistic regression, it is generally recommended to use an equal number of landslide and non-landslide points (Süzen and Doyuran 2004; Yesilnacar and Topal 2005; Nefeslioglu et al. 2008). Moreover, approximately 20 % of the dataset should be used to validate the results (Van Den Eeckhaut et al. 2006).

In a first step, for the Wenchuan earthquake landslide inventory 2,238 random sample locations were chosen from the landslide-free area to represent the absence of

Fig. 4 Land-use map of the study area
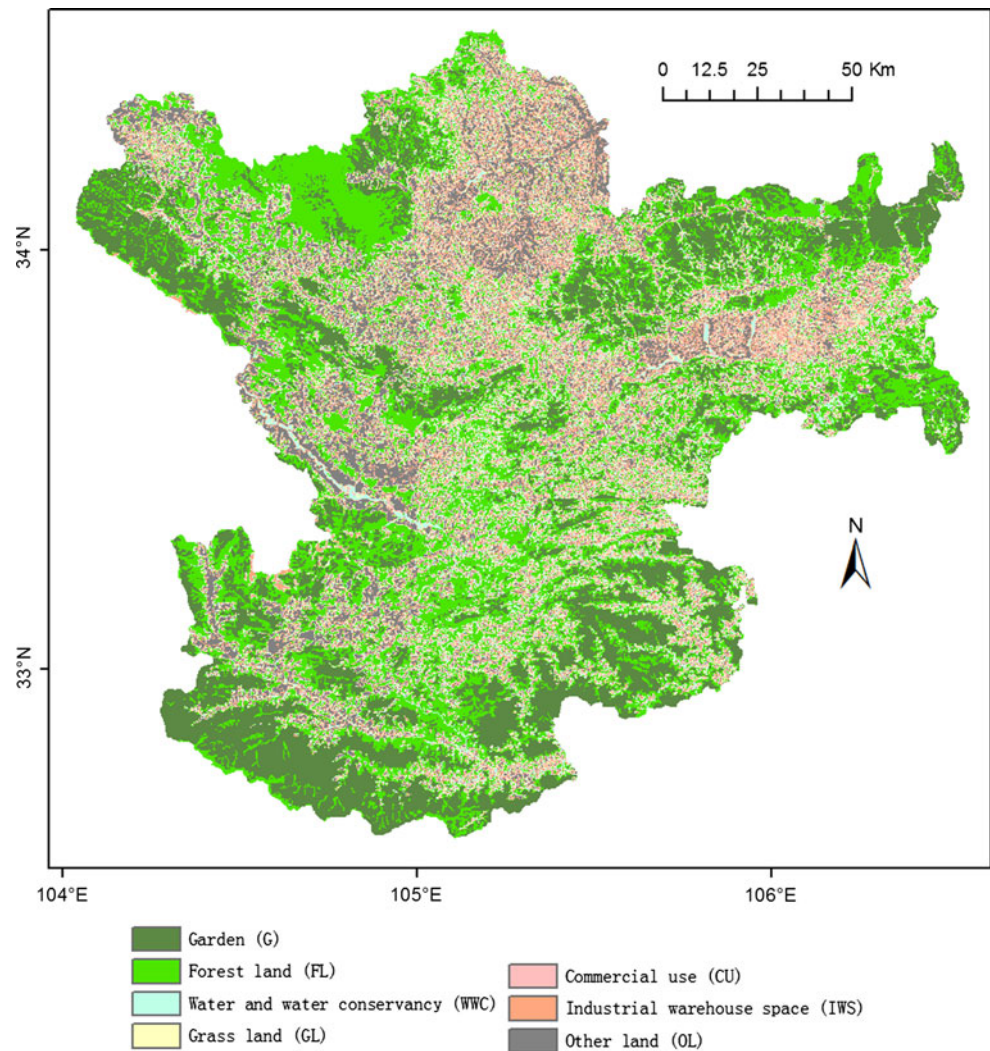
landslide. The 2,238 landslide pixels and 2,238 landslide-free pixels were merged and a new column of a binary variable indicating the presence and absence of landslides was added. The sample of 4,476 pixels was subdivided into calibration and validation data subsets. The calibration dataset contained 80 % of the pixels and the validation set the remaining 20 % of the pixels. Continuous data like topographical parameter data, PGA, and the distance to vector layer were handled in logistic regression analysis in their original format, in order not to alter the state and information present in the parameter maps. The rock groups, land use and aspect were categorized into a binary format (a dummy variable).

In a second step, the tolerance factor (TOL) and variance inflation factor (VIF) indexes of the causative factors for the Wenchuan earthquake-triggered landslide were calculated. Indexe values of VIF were found to be less than 2 and higher than 0.4 for the TOL 4 and were subsequently as input to the logistic analysis.

In the third step, all the causative factors multi-temporal landslide and the Wenchuan earthquake-triggered landslide were separately imported into the logistic regression algorithm with statistical packages for SPSS 15.0 for Windows to calculate the correlation of landslides to each factor. A forward stepwise logistic regression was carried out to incorporate only those predictor variables with a significant contribution to the presence of landslides. In this study, the significance level of score χ^2 for entering the model was 0.15. The significance level of Wald χ^2 for a variable to stay was 0.05.

In a fourth step, the landslide occurrence probability was computed using the logistic regression coefficients. Many methods described in literature divide the histogram of the susceptibility map into different categories (Guzzetti et al. 1999; Dai and Lee 2002; Ohlmacher and Davis 2003; Süzen and Doyuran, 2004; Ayalew et al. 2005). In this study, standard ArcGIS 9.3 tools were used to generate

Fig. 5 Peak ground acceleration contour map of the study area
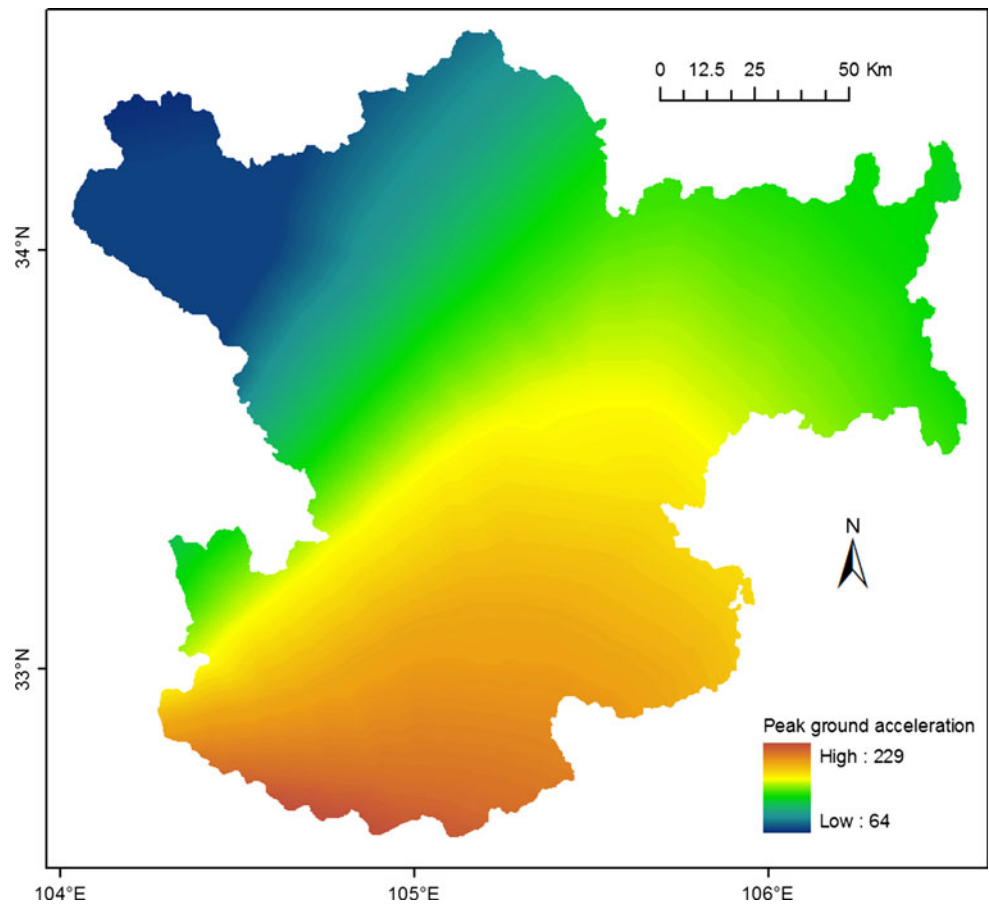
equal interval class breaks. The susceptibility map was divided into five classes: very low, low, medium, high, and very high.

Accuracy assessment

The correct classification percentage calculation was performed for the validation dataset to evaluate the performance of this generalization of the models constructed during the training stages. For this, the area under receiver-operating characteristic (ROC) curve (AUC) was applied, which constitutes one of the most commonly used accuracy statistics for the prediction models in natural hazard assessments (Begueria 2006).

According to Can et al. 2005, in the susceptibility value spatial distribution on a useful landslide susceptibility map, the observed landslide areas should coincide with those areas having high susceptibility values (Rule I). In addition, high susceptibility values should cover only small areas (Rule II). Since, in this study, only one pixel of each landslide was used to produce a landslide susceptibility map, the percentage of landslide number was used on each susceptibility level.

Results

Influence of pre-conditioning factors and landslides

The changes of landslide susceptibility due to the 2008 Wenchuan earthquake were investigated to understand the different impact of the multi-temporal landslide and the Wenchuan earthquake landslide. The authors were especially concerned with (1) the variations between landslide spatial distribution and pre-conditioning factors using the landslide proportion (LP) and (2) the variations of the landslide density (LD).

Lithology

The statistical analysis of landslide distribution with lithological data showed that the unit of phyllite, slate, and thin limestone was the most affected, with the unit of thick layer of limestone and slate being the second (Fig. 6a). Almost half of all earthquake-triggered landslides occurred in areas with phyllites, slates, and thin limestone, which however experienced with a relatively low landslide density of 0.095 landslides/km^2. The highest density (0.17

landslides/km^2) was found in areas with rock sand and gravel. The absence of landslides in units of magmatic rocks is mainly due to the small number of such cells, which together cover less than 0.0087 % of the total surface area.

Distance to faults

The comparison of landslide distribution with the distance to geological faults shows a general trend of a higher number of landslides with a shorter distance to faults. 55.45 % of landslide occurred within the distance of 2,100 m from faults (Fig. 6b). The greatest density (0.112 landslides/km^2) was found within the distance of 300 m from faults.

Topography

The majority (over 84.09 %) of all earthquake-triggered landslides occurred at elevations below 1,900 m, and of these more than 60 % were triggered at elevations from 1,300 to 1,900 m. Only 3.04 % of all earthquake-triggered landslides took place at elevations of over 2,500 m. Both the LP and the LD decrease with the elevations increase (Fig. 6c).

The relationship between landslides and the corresponding slope categories has been examined as shown (Fig. 6d). Landslides increase as the slope increases, until the maximum is reached in the 20°–30° category, and then generally decrease as the slope increases. Approximately 30 % of all earthquake-triggered landslides are located on slopes with angles between 20° and 30°. The highest landslide density was found for areas with slope angles of over 50°. This could be related to the amplification effect of the ridges and the transitional and turning position of gentle topographic slope to steep slope positions was the most seismic ground striking (Huang and Li 2008).

The influence of aspect on landslides was also analyzed. Both the LD and the LP have a slightly higher value in S direction than in any others (Fig. 6e), which may indicate that slope aspect has a minor influence on the distribution of earthquake landslides.

Distance to rivers

The statistical analysis showed that a strong relation could be observed between landslide distribution and the distance to rivers. Over 67.92 % of earthquake-triggered landslides occurred within a distance of 1,000 m from rivers. Both the LP and the LD decrease with a longer distance from rivers (Fig. 6f).

Land-use

The statistical analysis showed that the vast majority of earthquake landslides occurred in areas classified as forest land (42.05 %) and other land used for agricultural production or irrigation or Saline land (39.32 %), while all other classes experienced less than 20 % of all landslides (Fig. 6g).

Mapping of landslide susceptibility

A forward stepwise logistic regression was carried out. The variables aspect, elevation, slope, land-use, rock groups, PGA, and distance to faults were selected due to their statistical significance. After the landslide occurrence probability was computed using the logistic regression coefficients, the re-classified susceptibility map created by the described methodology is presented in Fig. 7. Table 3 shows the distribution of the five susceptibility zones.

Accuracy assessment

The predicted accuracies of the validation dataset were 72.3 % for landslides and 68.9 % for non-landslides, with an average value of 70.6 %. Again, a high AUC value of 0.777 was reached.

As in this study only one pixel of each landslide was used to produce a landslide-susceptibility map, the percentage of landslide numbers was used without using observed landslide areas on each susceptibility level. The percentage of the area covered by the very low and low susceptibility zones was found to be relatively large, with a value of 43.11 %. Still, the very low and low susceptibility area included about 15 % of all the landslides. The percentage of the area computed with the highest susceptibility and of the landslide numbers was 14.25 and 40.8 %, respectively.

Conclusions

The high landslide susceptibility is related to the soft and erodible lithologic formations and the high tectonic activity. In combination with other factors, this causes geological disasters with a very high magnitude and frequency of landslides and debris flows. The Wenchuan earthquake mobilized large amounts of material and weakened the geological structure in Longnan, making it more susceptible for future slope failures. It is a challenge for the many tens of millions of people who live in this region. In the past 10 years, several large landslide disasters have occurred. For example, the Gansu mudslide took place on August 8th 2010 within the Longnan region. It was caused by heavy rainfall of 77.3 mm in 1 h and killed more than 1,287 people (Yu et al. 2010). In addition, the increase of urbanization, the building of new infrastructure such as new highways and high-speed railway lines (Chen et al.
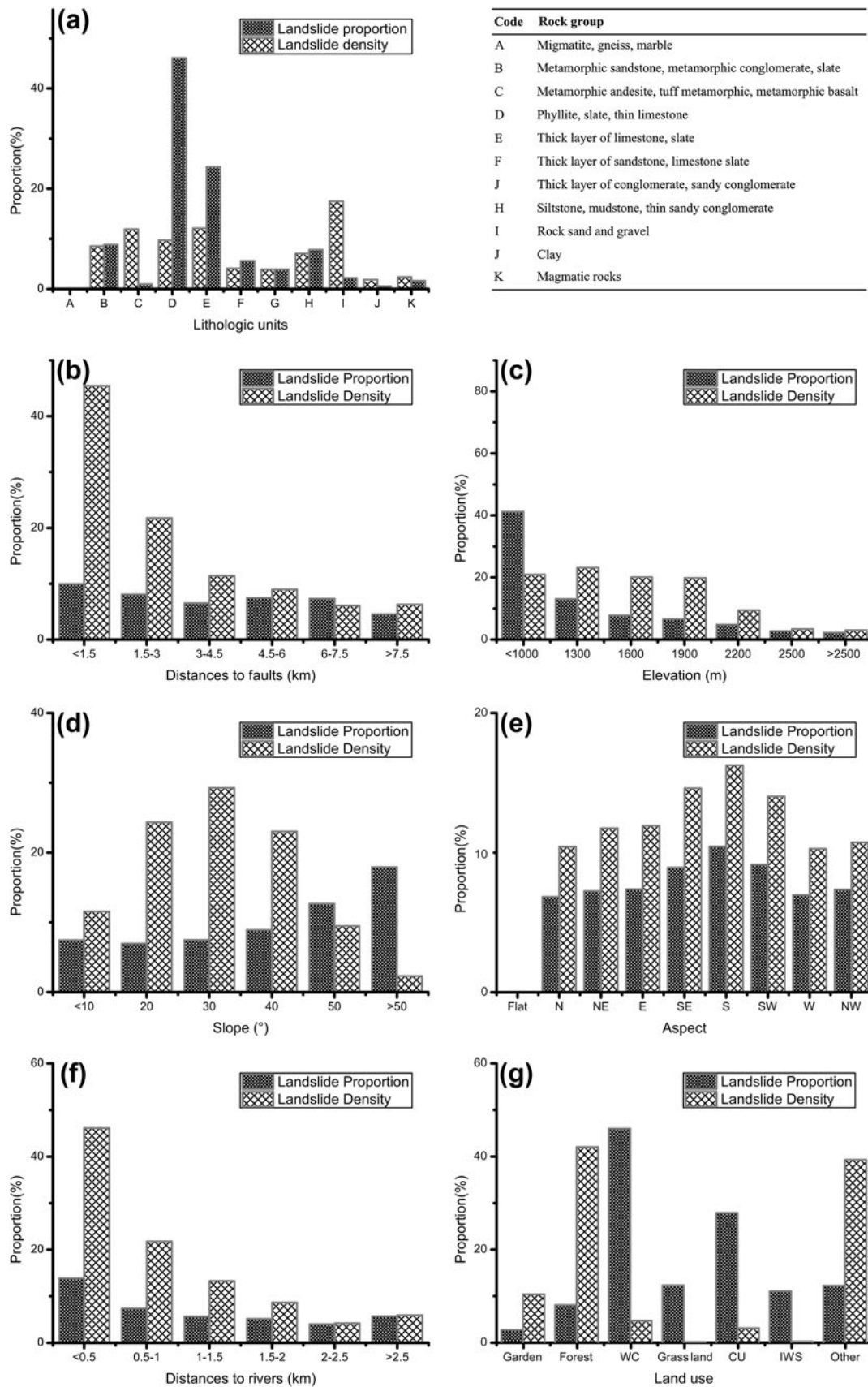
Fig. 6 Histogram of landslides and pre-disposing factors (LD and the LP value is enlarged 100 times)
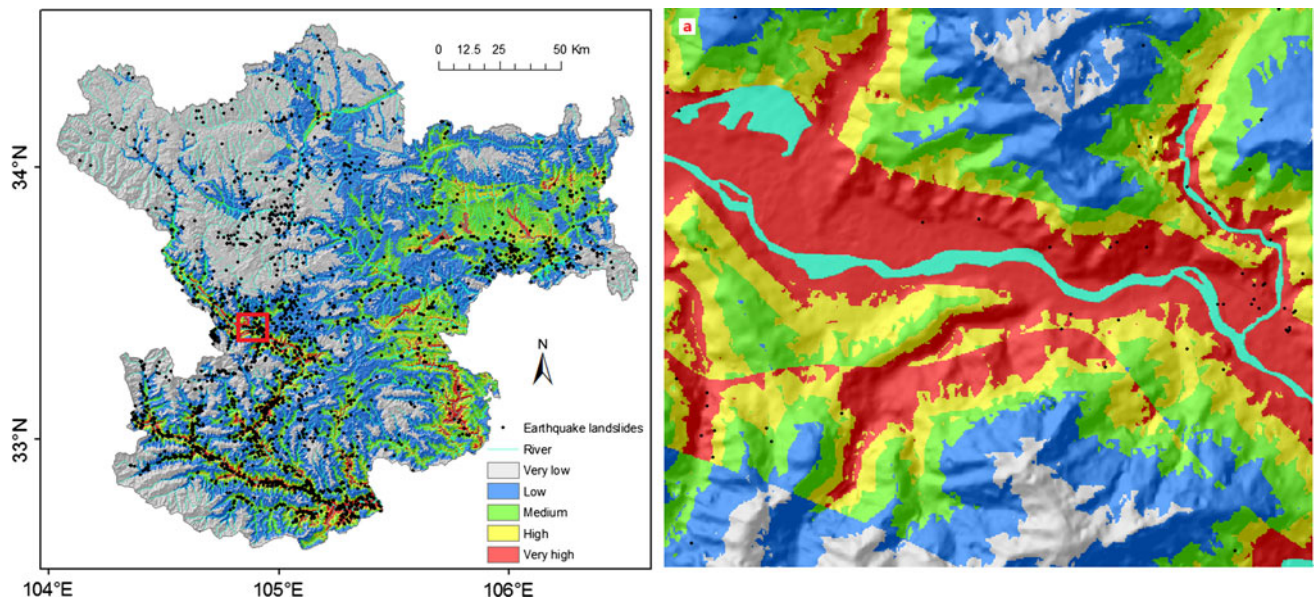
Fig. 7 Re-classification susceptibility map of logistic regression analysis

Table 3 The distribution of four susceptibility zones in the study area

Susceptibility class	Reclassified value	% Area covered	% Landslide number
Very low	0–0.2	15.85	3.71
Low	0.2–0.4	27.26	11.39
Medium	0.4–0.6	22.76	16.40
Very high	0.6–0.8	19.88	27.70
High	0.8–0.991	14.25	40.80

2006), and the reconstruction following the Wenchuan earthquake increased the negative consequences of landslide occurrences, and also accelerated the impact of landslides on society. Therefore, landslides in the Longnan of China have received considerable attention after Wenchuan earthquake; 55.45 % of all earthquake-triggered landslides occurred in areas with phyllites or slates and occurred within the distance of 2,100 m from faults; 67.92 % of them occurred within a distance of 1,000 m from rivers. More than 60 % were triggered at elevations from 1,300–1,900 m and approximately 30 % of all earthquake-triggered landslides were located on slopes with angles between 20° and 30°. The slope aspect, however, has a minor influence on the distribution of earthquake landslides. The majority of earthquake landslides occurred in areas classified as forest land (42.05 %).

In order to predict areas most likely to experience slope failures in the future, landslide susceptibility maps have to be created. Nevertheless, the exact timing of future landslides cannot be estimated accurately with the current methodologies, given the complex nature of the respective processes. A susceptibility map shows where landslides may occur. The landslide susceptibility map ranks the slope stability of the study area in categories that range from stable to unstable. There are many GIS-based qualitative and quantitative techniques available to analyze the relationship between landslides and environmental factors. In this study, a logistic regression model was presented within the GIS framework for landslide susceptibility calculation. The aspect, elevation, slope, land use, rock groups, PGA, and distance to fault were the most significant factors to estimate Wenchuan earthquake-triggered landslide susceptibility. The final susceptibility map shows areas that are highly prone to earthquake-triggered landslides in the future, assuming that the epicenter is roughly in the same region. A landslide susceptibility map is fundamental in quantifying risk due to earthquake-triggered landslides in the Longnan region. The calculated landslide susceptibility map could be used for spatial and emergency planning by Longnan authorities.

References

Aleotti P, Chowdhury R (1999) Landslide hazard assessment: summary review and new perspectives. Bull Eng Geol Environ 58:21–44

Atkinson PM, Massari R (1998) Generalized linear modeling of susceptibility to landsliding in the central Apennines, Italy. Comput Geosci 24:373–385

Ayalew L, Yamagishi H, Marui H, Kanno T (2005) Landslides in Sado Island of Japan Part II. GIS-based susceptibility mapping with comparisons of results from two methods and verifications. Eng Geol 81:432–445

Bai SB, Wang J, Lü GN, Zhou PG, Hou SS, Xu SN (2010) GIS-based logistic regression for landslide susceptibility mapping of the Zhongxian segment in the Three Gorges area, China. Geomorphology 115:23–31

Bai SB, Lu GN, Wang J, Ding L, Zhou PG (2011) GIS-based rare events logistic regression for landslide susceptibility mapping of Lianyungang, China. Environ Earth Sci 3(25):1–11

Begueria S (2006) Validation and evaluation of predictive models in hazard assessment and risk management. Nat Hazards 37(3):315–329

Bell R, Glade T (2004) Quantitative risk analysis for landslides—examples from Bdudalur, NW-Iceland. Natural Hazard and Earth System Science 4(1):117–131

Brabb EE (1984) Innovative approaches to landslide hazard and risk mapping. Proceeding of Fourth International Symposium on Landslides, vol 1. Canadian Geotechnical Society, Toronto, pp 307–324

Can T, Nefeslioglu HA, Gokceoglu C, Sonmez H, Duman TY (2005) Susceptibility assessments of shallow earthflows triggered by heavy rainfall at three subcatchments by logistic regression analyses. Geomorphology 72:250–271

Chacon J, Irigaray C, Fernandez T, El Hamdouni R (2006) Engineering geology maps: landslides and geographical information systems. B Eng Geol Environ 65:341–411

Chen WW, Zhai ZF, Liu G, Liang SY (2006) The engineering geological problems of the Gansu section of Lanzhou-Haikou highway. Lanzhou University Press, Lanzhou

China Geological Survey Bureau of Statistics (2008) Geological Bulletin of China, China Geological Environmental InfoNet. Available online at: http://www.cigem.gov.cn/defaulteng.html. Accessed 23 May 2009

Chung CJF, Fabbri AG (1999) Probabilistic prediction models for landslide hazard mapping. Photogramm Eng Remote Sens 65:1389–1399

Chung CF, Kojima H, Fabbri AG (2002) Stability analysis of prediction models for landslide hazard mapping. In: Allison RJ (ed) Applied geomorphology: theory and practice. John Wiley and Sons, London, pp 1–19

Cruden DM, Varnes DJ (1996) Landslide types and processes. In: Turner AK, Schuster RL (eds) Landslides: investigation and mitigation (Special Report). National Research Council, Transportation and Research Board Special Report 247. Washington, DC, pp 36–75

Cui P, Wei FQ, He SM, You Y, Chen XQ, Li ZL, Dang C, Yang CL (2008) Mountain disasters induced by the earthquake of May 12 in Wenchuan and the disasters mitigation (In Chinese). J Mt Sci 26(3):280–282

Cui P, Zhu YY, Han YS, Chen XQ, Zhuang JQ (2009) The 12 May Wenchuan earthquake-induced landslide lakes: distribution and preliminary risk evaluation. Landslides 6:209–223

Dai FC, Lee CF (2002) Landslide characteristics and slope instability modeling using GIS Lantau Island, Hong Kong. Geomorphology 42:213–238

Dai FC, Lee CF, Li J, Xu ZW (2001) Assessment of landslide susceptibility on the natural terrain of Lantau Island, Hong Kong. Environ Geol 40:381–391

Dai FC, Xu C, Yao X, Xu L, Tu XB, Gong QM (2011) Spatial distribution of landslides triggered by the 2008 Ms 8.0 Wenchuan earthquake, China. J Asian Earth Sci 40:883–895

Derbyshire E, Meng X, Billard A, Muxart T, Dijkstra TA (2000) The environment: geology, geomorphology, climate and land use. In: Derbyshire E, Meng XM, Dijkstra TA (eds) Landslides in the thick loess terrain of North-west China. Wiley, Chichester, pp 21–46

Fell R, Cororninas J, Bonnard C, Cascini L, Leroi E, Savage WZ (2008) Guidelines for landslide susceptibility, hazard and risk-zoning for land use planning. Eng Geol 102:85–98

Guzzetti F, Carrara A, Cardinali M, Reichenbach P (1999) Landslide hazard evaluation: a review of current techniques and their application in a multi-scale study, central Italy. Geomorphology 31:181–216

Guzzetti P, Reichenbach M, Cardinali M, Galli F, Ardizzone F (2005) Landslide hazard assessment in the Staffora basin, northern Italian Apennines. Geomorphology 72:272–299

Huang RQ, Li WL (2008) Development and distribution of geohazards triggered by the 5.12 Wenchuan Earthquake in China. Sci China Ser E-Tech 52(4):810–819

Longnan Bureau of Land and Resources (2008) The recovery and reconstruction of geological disaster prevention special plan at Longnan of Gansu Province (in Chinese)

Lu DL, Cui JW, Li XJ, Lian WP (2010) Ground motion attenuation of M_s8.0 Wenchuan earthquake. Earthquake Sci 23:95–100

Nefeslioglu HA, Duman TY, Durmaz S (2008) Landslide susceptibility mapping for a part of tectonic Kelkit Valley (Eastern Black Sea region of Turkey). Geomorphology 94:410–418

Ohlmacher CG, Davis CJ (2003) Using multiple regression and GIS technology to predict landslide hazard in northeast Kansas, USA. Eng Geol 69:331–343

Qin XW, Yang JZ, Zhang Z, Huang H, Yu DQ, Chen YP, Zhang G, Gu YQ (2009) Remote sensing emergency survey in Wenchuan earthquake area. The science press of China (in Chinese), China

Scheidegger AE, Ai NS (1987) Clay slides and debris flow in Wudu region. J Soil Water Conserv 1(2):19–27

Soeters R, van Westen CJ (1996) Slope instability recognition analysis and zonation. In: Turner KT, Schuster RL (eds) Landslides: Investigation and Mitigation. Transportation Research Board National Research Council, Special Report. Washington, DC, pp 129–177

Süzen ML, Doyuran V (2004) A Comparison of the GIS based landslide susceptibility assessment methods: multivariate versus bivariate. Environ Geol 45:665–679

Tang C, Zhu J, Li WL, Liang JT (2009) Rainfall-triggered debris flows following the Wenchuan earthquake. Bull Eng Geol Environ 68:187–194

Van Den Eeckhaut M, Vanwalleghem T, Poesen J, Govers G, Verstraeten G, Vandekerckhove L (2006) Prediction of landslide susceptibility using rare events logistic regression: a case-study in the Flemish Ardennes (Belgium). Geomorphology 76:392–410

Van Westen CJ, Getahun FL (2003) Analyzing the evolution of the Tessina landslide using aerial photographs and digital elevation models. Geomorphology 54:77–89

Van Westen CJ, Castellanos E, Kuriakose SL (2008) Spatial data for landslide susceptibility, hazard, and vulnerability assessment: an overview. Eng Geol 102:112–131

Varnes DJ (1984) Landslide hazard zonation: a review of principles and practice, IAEG Comission on Landslides and other Mass Movements. UNESCP Press, Paris, p 63

Xie H, Zhong DL, Jiao Z, Zhang JS (2009) Debris flow in Wenchuan quake-hit area in 2008 (In Chinese). J Mt Sci 27(4):501–509

Xu C, Xu X, Lee YH, Tan X, Yu G, Dai F (2012a) The 2010 Yushu earthquake triggered landslide hazard mapping using GIS and weight of evidence modeling. Environ Earth Sci 66(6):1603–1616. doi:10.1007/s12665-012-1624-0

Xu C, Xu X, Dai F, Saraf AK (2012b) Comparison of different models for susceptibility mapping of earthquake triggered

landslides related with the 2008 Wenchuan earthquake in China. Comput Geosci 46:317–329

Yalcin A, Reis S, Aydinoglu AC, Yomralioglu T (2011) A GIS-based comparative study of frequency ratio, analytical hierarchy process, bivariate statistics and logistics regression methods for landslide susceptibility mapping in Trabzon, NE Turkey. Catena 85:274–287

Yesilnacar E, Topal T (2005) Landslide susceptibility mapping: a comparison of logistic regression and neural networks methods in a medium scale study, Hendek region (Turkey). Eng Geol 79:251–266

Yin YP, Wang FW, Sun P (2009) Landslide hazards triggered by the 2008 Wenchuan earthquake, Sichuan, China. Landslides 6:139–152

Yu B, Yang YH, Su YC, Wang GF (2010) Research on the giant debris flow hazards in Zhouqu County, Gansu Province on August 7, 2010. J Eng Geol 18(4):437–444